ADAPTIVE FUSION OF MULTISOURCE RASTER DATA APPLYING FILTER TECHNIQUES

K. Steinnocher
Austrian Research Centers, Seibersdorf, Environmental Planning, A-2444 Seibersdorf, klaus.steinnocher@arcs.ac.at

KEYWORDS: Adaptive Filters, Image Fusion, Image Sharpening, Multiresolution Data, Pre-Segmentation.

ABSTRACT

Current remote sensors offer a wide variety of image data with different characteristics in terms of temporal, geometric, radiometric and spectral resolution. Although the information content of these images might be partially overlapping, the complementary aspects represent a valuable improvement for information extraction. To exploit the entire content of multisensor image data, appropriate techniques for image fusion are indispensable. The objective of this paper is to analyse the benefits that can be gained from the adaptive image fusion (AIF) method. This method allows the fusion of geometric (spatial) and thematic (spectral) features from multisource raster data using adaptive filter algorithms. If applied to multiresolution image data, it will sharpen the low spatial resolution image according to object edges found in the higher spatial resolution image. In contrast to substitution methods, such as Intensity-Hue-Saturation or Principal-Component Merging, AIF preserves the spectral characteristics of the original low resolution image. Thus, it supports applications that rely on subsequent numerical processing of the fused image, such as multispectral classification. However, it may also be used in combination with substitution merging methods leading to an improved product for visual interpretation. In this case, the AIF will be applied in order to sharpen the original low spatial resolution image before performing the substitution. From the various applications that could benefit from AIF, three examples are presented: improving the delineation of forest areas, sharpening of agricultural fields and monitoring of urban structures. In all cases, the fusion leads to an improved segmentation and a more precise estimation of the area of single land cover objects.

1. INTRODUCTION

Image fusion in a general sense can be defined as "the combination of two or more different images to form a new image by using a certain algorithm" (Van Genderen and Pohl, 1994). It aims at the integration of all relevant information from a number of single images into one new image. From an information science point of view, image fusion can be divided into three categories depending on the abstraction level of the images: pixel, feature and decision based fusion. On the pixel level, the fusion is performed on a per-pixel basis. This category encompasses the most commonly used techniques (Vrabel 1996). The second level requires the derivation of image features, which are then subject to the fusion process. Decision based fusion combines either pre-classified data derived separately from each input image or data from multiple sources in one classification scheme (Benediktsson and Swain, 1992, Schistad Solberg et al. 1994).

An alternative grouping of image fusion techniques refers to the different temporal and sensor characteristics of the input imagery. The combination of multitemporal - single sensor images represents a valuable basis for detecting changes over time (Singh, 1989, Weydahl, 1993, Kressler and Steinnocher, 1996). Multisensor image fusion combines the information acquired by different sensor systems, to benefit from the complementary information inherent in the single image data. A representative selection of studies on multisensor fusion, comprising a wide range of sensors, is given by Pohl and van Genderen (1998). Within this group, a focus can be found on the fusion of optical and SAR data (Harris et al., 1990, Schistad Solberg et al., 1994) and of optical image data with different spectral and spatial resolutions (Chavez et al., 1991, Pellemans et al., 1993, Shettigara, 1992, Zhukov et al., 1995, Garguet-Duport et al., 1996, Yocky, 1996, Vrabel, 1996, Wald et al. 1997).

In the remainder of this paper, we will concentrate on the fusion of multisensor optical image data with different spatial and spectral resolutions. High resolution data sets of this kind are typically acquired from single platforms carrying two sensors in the optical domain - one providing panchromatic images with a high spatial resolution, the other providing multispectral bands (in the visible and near infrared spectrum) with a lower spatial resolution. Current examples of these platforms are SPOT3/4, IRS-1C/D, and the just recently launched Landsat 7. For the near future a number of satellites with similar characteristics are announced (Carlson and Patel, 1997).

The motivation for merging a panchromatic with multispectral images lies in the increase of details while preserving the multispectral information. The result is an artificial multispectral image stack with the spatial resolution of the panchromatic image. Common methods to perform this task are arithmetic merging procedures or component substitution techniques such as the Intensity-Hue-Saturation (IHS) or the Principal Component Substitution procedures (Carper et al., 1990, Chavez et al., 1991, Shettigara, 1992). These techniques are valuable for producing improved image maps for visual interpretation tasks, as they strongly enhance textural features. On the other hand, they can lead to a significant distortion of the radiometric properties of the merged images (Vrabel, 1996). Pellemans et al. (1993) introduced the radiometric method, where the new multispectral bands are derived from a linear combination of multispectral and panchromatic radiances. While this method keeps the radiometry of the spectral information, it

is restricted to bands that are spectrally located within the spectral range of the panchromatic image. An interesting approach has been presented by Zhukov et al. (1995), which is based on the retrieval of spectral signatures, which correspond to constant grey levels in the panchromatic image. The result reveals sub-pixel variations in the multispectral bands, which are associated with grey level variations in the panchromatic image. Most promising are methods that use wavelet transforms for fusion of multiresolution images, as they preserve the spectral characteristics of the fused image to a high extent (Ranchin and Wald, 1993, Garguet-Duport et al., 1996, Yocky, 1996, Wald et al., 1997). In this paper, we will present an alternative method that is based on adaptive filters.

2. METHODOLOGY

Fusion of multiresolution optical image data aims at the derivation of multispectral images providing the high spatial resolution of the panchromatic image. The perfect result of such a process would be an image, that is identical to the image the multispectral sensor would have observed if it had the high resolution of the panchromatic sensor (Wald et al., 1997). Such an image would allow differentiating at least all objects that are detectable in the panchromatic image. An approximation of the desired result could be obtained by first extracting the objects from the panchromatic image and „filling" them with the corresponding average multispectral information. Similar techniques have been successfully used for integrating spectral image data with vector layers in a GIS (Janssen et al., 1990). The drawback of this method for multi-image fusion lies in the requirement of a consistent set of object borders. Although the requirement can be fulfilled through segmentation of the panchromatic image, it would need computationally intensive and therefore time consuming preprocessing. As an alternative, we propose a filtering approach, called Adaptive Image Fusion (AIF), that uses local object edges instead of image segments.

2.1. Sigma filter

We assume that an image object Z is represented by a set of neighbouring pixels z_i, whose values are Gaussian distributed, i.e. $z \sim N(\mu_Z, \sigma_Z)$. This assumption of normality is generally reasonable for common spectral response distributions (Lillesand and Kiefer, 1994). In the local neighbourhood of an object edge we will therefore find two distributions, each representing one of the neighbouring objects. To separate these objects, i.e. to assign each pixel to one of these objects, adaptive filter techniques can be used. These filters have been successfully applied to image data for noise reduction, in particular for suppression of speckle in SAR imagery. We have chosen a modified sigma filter as it matches the assumptions given above.

The sigma filter averages only those pixels in a local window, which lie in a two-sigma range of the central pixel value (Lee 1983). All other pixels are assumed to belong to another distribution i.e. they represent a neighbouring object. As this filter is based on the assumption that the central pixel is in fact the mean of its Gaussian distribution, it might not include all relevant pixels in the averaging process. Therefore, a more general approach, namely the modified sigma filter, was presented by Smith (1996). It averages all pixels, which could belong to the same distribution as the central pixel without knowing the actual mean of this distribution.

Application of the modified sigma filter requires the estimation of the normalised standard deviation which can be based on empirical analysis of the panchromatic image (Smith 1996). First, a local average and a local standard deviation image are computed from the original image, using the window size chosen for the filter process. Next, the standard deviation image is divided by the average image on a pixel basis resulting in a normalised standard deviation image. The mode of the histogram of this image is an adequate estimate to start with, although test runs have shown that in most cases it has to be reduced to get the desired results.

When applying the modified sigma filter, areas with a low standard deviation, i.e. areas containing one object, will be smoothed. Within areas of high standard deviation, i.e. areas containing object edges, only those pixels will be averaged that belong to the same distribution as the central pixel.

2.2. Adaptive image fusion

For the fusion approach, the multispectral bands are included in the filtering process. As most fusion techniques, AIF requires co-registration of the panchromatic and the multispectral images and nearest neighbor resampling of the multispectral bands to the higher spatial resolution. There is no need of applying a higher level resampling process, such as cubic interpolation, as the blockiness of the lower resolution images will be eliminated during the fusion process. In the following, the new high resolution pixels of the multispectral bands are addressed as sub-pixels.

The AIF algorithm starts with applying a modified sigma filter to the panchromatic image. At each position of the moving window the two sigma range related to the central pixel is calculated, and all pixels within the window which fall into that range are selected. The position of the selected pixels is then transferred to the multispectral band, where the averaging of the respective sub-pixels is performed. The process could be described as sigma filtering of the multispectral band where the filter behavior is controlled by the panchromatic image. It is important to note that no spectral information is transferred from the panchromatic image to the multispectral band during the whole procedure. This leads to a better delineation of objects in the multispectral band without significantly changing the spectral information.

The effect of the AIF is shown in Figure 1. The figure on the left side represents an (idealised) panchromatic image, the figure in the center the respective (idealized) multispectral band. It is obvious that the spectral correlation between the two images is relatively low (as occurs e.g. with a panchromatic image and a near infrared channel). By applying the AIF iteratively, the mixed pixels of the multispectral band will be separated step by step into the single objects they are composed of. The right

figure shows an (idealized) output of the fusion process, where the shape of the objects is identical with the panchromatic image, but the spectral behavior of the objects corresponds to the multispectral image.

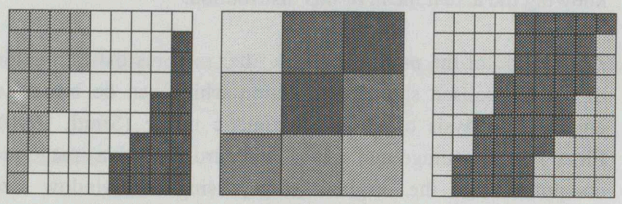

Fig. 1. Effect of Adaptive Image Fusion: (a) panchromatic image ; (b) multispectral image ; (c) fused multispectral image.

Although AIF sharpens the multispectral image according to object edges found in the panchromatic image, this effect is limited to object edges that occur both in the panchromatic and the multispectral image. Edges appearing only in the panchromatic image will cause no significant effect in the multispectral band, while edges in the multispectral band that do not show up in the panchromatic image will get slightly blurred. Objects that are smaller than the original multispectral pixel size will only be sharpened, if their spectral reflectance is significantly different from their local environment. At the same time as object edges are sharpened, the area within an object will be smoothed. This effect can be seen as a pre-segmentation of the multispectral image. It reduces the occurrence of mixed pixels, thus improving the quality of a subsequent classification.

3. APPLICATION

3.1. Agricultural case study

The AIF algorithm was first applied to a multisensor image acquired by the Indian remote sensing satellite IRS-1C. This system provides panchromatic images with a spatial resolution of 5.6m (PAN), and three multispectral bands (green, red and near infrared) with a resolution of 23.5m (LISS-2/3/4). The commercially available scenes are radiometrically preprocessed, panorama corrected and resampled to a pixel size of 5m and 25m respectively. The acquired scene (path 30, row 35, quadrant A) was sensed on August 9, 1996 and covers an area of approximately 70x70 km^2 located in Upper Austria (centered on 13°35'E / 47°58'N). The images were geocoded to the Austrian reference system (Gauß-Krüger M31). The multispectral bands were resampled to 5m pixel size to match the resolution of the panchromatic image.

Application of AIF requires the selection of two parameters, the normalised standard deviation and the size of the local window. The former can be estimated from the panchromatic image as described in section 2.1 The minimum size of the local window is the ratio between original multispectral and panchromatic pixel size. This minimum size offers the advantage of short computation time. However, test runs of AIF have shown that larger window sizes, such as 9x9 or 11x11, lead to significantly better results. This will increase the computation time of the program, but at the same time will reduce the number of iterations. This is due to the stronger effect of averaging, when larger window sizes are used.

For the demonstration study a normalized standard deviation of 0.01 and a window size of 11x11 were chosen. Each multispectral band was fused subsequently with the panchromatic image, thus leading to a synthetic multispectral image stack. Being the most commonly used merging technique, an IHS procedure was performed for comparison.

Visual evaluation of the fusion results shows the differences between AIF and IHS merging (Fig. 2). The impression of the AIF image is that of a pre-segmented image, where the variation of grey levels within the objects is very low, while the objects are clearly separated from each other. Areas with a high variance in the panchromatic image, such as the village left of the center, appear like one homogenous object in the fused image. The IHS image has more textural information that supports visual interpretation, but also distorts the spectral information significantly, as can be seen in some of the agricultural fields.

Multispectral classification of the fused images confirms the different effects (Fig. 3). A comparison of the classification of the original image and the AIF image, both classified with the same set of spectral signatures, shows the similar pattern of assigned classes. The delineation of objects is significantly better in the AIF image, and it contains less single pixel objects. Classification of the IHS image was performed with a different set of spectral signatures, as the spectral distortions did not allow using the signatures from the original multispectral image. The appearance of the classification is noisier, and in some areas differs significantly from the original classification.

Quality assessment. The assessment focuses on how much the radiometry of the multispectral images is distorted by the fusion procedure. It is based on the idea that a synthetic image once degraded to its original resolution should be as identical as possible to the original image. This property is estimated by comparing the mean values and standard deviations of and the correlation coefficients between the degraded and the original images (Wald et al., 1997). In order to produce the degraded images, the fusion results were averaged applying a 5x5 filter kernel and resampled to 25m pixel size. Table 1 presents the results of the comparison between the degraded images and the original data. The first column shows the global mean (μ) and standard deviation (σ) of the original multispectral bands. The columns entitled AIF and IHS give the respective values of the merged products.

The results of AIF show no significant differences in the mean values, but the standard deviation is slightly reduced. This is due to the averaging performed during the merging process. IHS merged images show a higher deviation in the mean values and an increase of the standard deviation resulting from the inclusion of textural information from the panchromatic image. It is interesting to note, that for channel 4 (NIR) the standard deviation has decreased during the IHS merge.

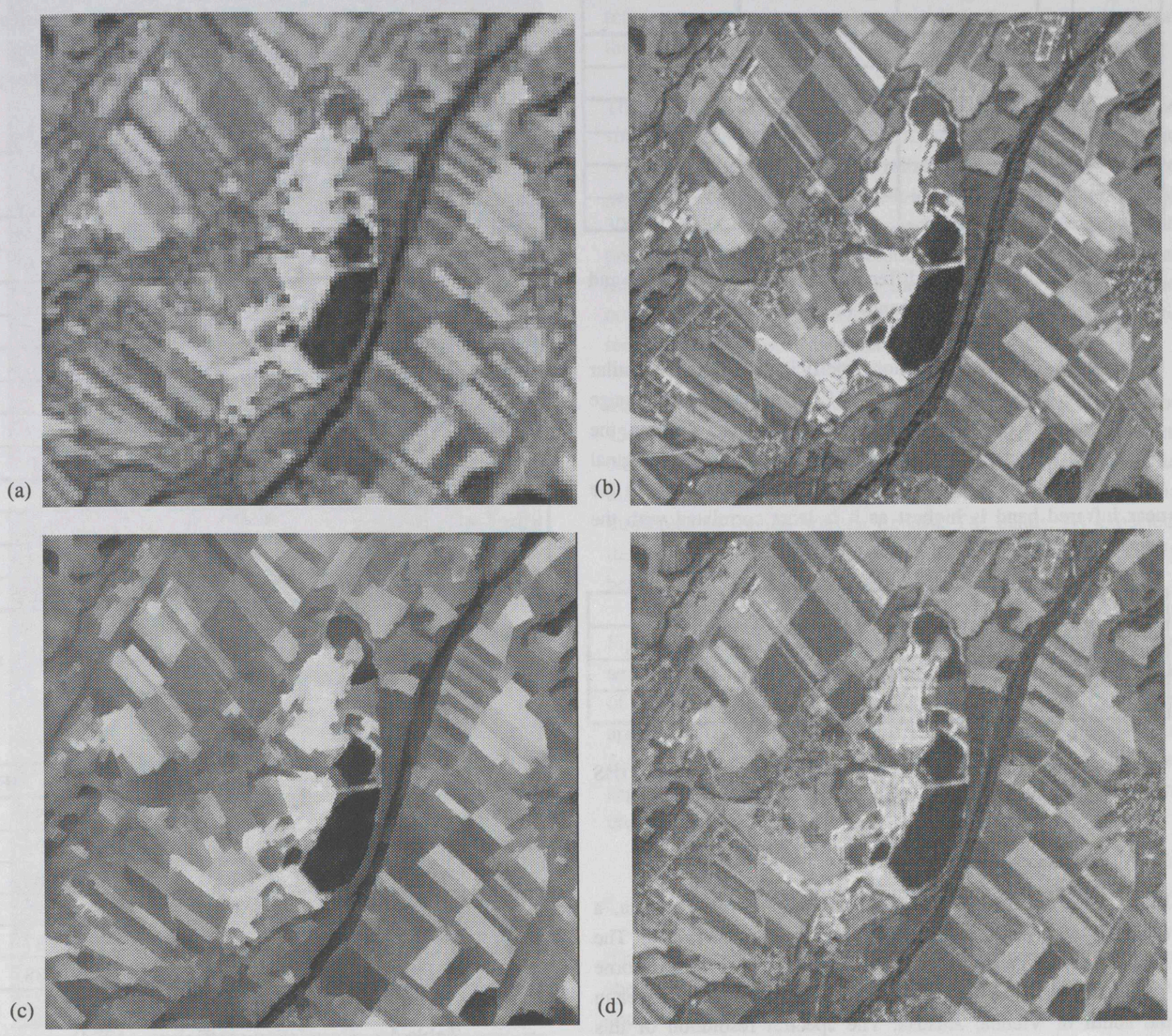

Fig. 2. Comparison of Fusion techniques. (a) original multispectral image. (b) panchromatic image. (c) result of AIF. (d) result of IHS merging. (© Euromap 1997)

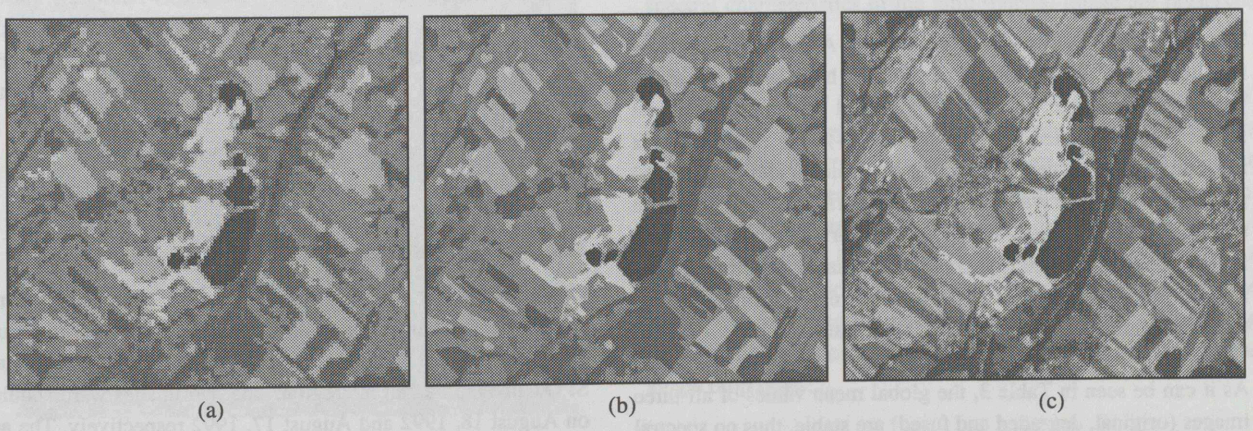

Fig. 3. Multispectral classification based on (a) original image, (b) AIF image, and (c) IHS image.

Image bands		Original image	AIF	IHS
LISS-2	μ	89.6	89.6	91.1
green	σ	21.7	21.0	26.0
LISS-3	μ	32.1	32.0	33.0
red	σ	13.0	12.6	14.8
LISS-4	μ	100.6	100.8	99.4
NIR	σ	26.1	23.6	20.1

Table 1. Statistics of differences between original and degraded image bands (IRS-1C).

Comparison of the correlation coefficients leads to similar results (see Table 2). It can be clearly seen that the AIF image bands correlate highly with the original data, whereas the correlation between the IHS merged image and the original image is significantly lower. As expected, the difference in the near infrared band is highest as it is least correlated with the panchromatic image.

Bands	AIF	IHS
LISS-2	0.99	0.92
LISS-3	0.99	0.97
LISS-4	0.97	0.85

Table 2. Correlation coefficients between AIF and IHS merged images with the original ones (IRS-1C).

3.2. Urban case study

In order to evaluate the AIF on very high resolution data, a second study was performed on airborne scanner data. The image was acquired by a Daedalus AADS 1268 ATM (Airborne Thematic Mapper) scanner in August 1991 and covers an area in the south of Vienna, Austria. The spectral resolution of this scanner comprises 11 bands. For the case study only the 6 bands that correspond to the spectral bands of Landsat TM were used. The scanner data were geocoded to the Austrian reference system (Gauß-Krüger M34) with a spatial resolution of 6m.

The focus of this study was an analysis of AIF results compared to multispectral images observed with the high resolution of the panchromatic image. In order to perform this comparison the ATM image (denoted by org in Table 4) was degraded to a resolution of 18m (denoted by deg in Table 4) and an artificial panchromatic image was computed by averaging bands 1 to 4 on the 6m pixel basis. Next, an AIF was performed on the degraded image bands and the panchromatic image resulting in an artificial image stack with a resolution of 6m. This image stack was then compared to the original image data.

As it can be seen in Table 3, the global mean values of all three images (original, degraded and fused) are stable, thus no spectral distortion occurred during the fusion process. Again the standard deviation of the degraded and the fused image is lower than the one of the original image. For more detailed analysis the correlation between the three image stacks were computed (see Table 4). Whereas the correlation between the original image and the degraded image lies between 0.82 and 0.85, the correlation between the original and the AIF is significantly higher except for band 5. This effect might be due to the fact that the correlation between the multispectral and the panchromatic image is lowest for band 5.

Image bands		Original image	Degraded image	AIF image
ATM 1	μ	85.3	85.4	85.1
blue	σ	27.3	19.5	19.9
ATM 2	μ	56.3	56.3	56.2
green	σ	19.5	14.1	14.5
ATM 3	μ	51.2	51.2	51.0
red	σ	24.2	18.0	18.5
ATM 4	μ	67.5	67.6	67.7
NIR	σ	21.7	15.7	16.0
ATM 5	μ	69.2	69.1	69.3
NIR	σ	27.3	21.0	20.0
ATM 6	μ	71.6	71.5	71.4
MIR	σ	31.7	23.7	23.6

Table 3. Statistics of differences between original and degraded image bands (ATM).

Bands	org - deg	org - AIF	deg - AIF
ATM 1	0.82	0.94	0.87
ATM 2	0.83	0.94	0.88
ATM 3	0.84	0.94	0.89
ATM 4	0.82	0.93	0.82
ATM 5	0.85	0.84	0.87
ATM 6	0.84	0.89	0.88

Table 4. Correlation coefficients (ATM).

A visual comparison shows the benefits and limitations of the AIF (Fig. 4). Compared to the degraded image, the fused image is clearly sharper and shows no blockiness. Although most of the object structures seen in the original image will be found in the fused image as well, some of the smaller objects are blurred (e.g. garden area in the upper left part of the image, single buildings in the village in the lower part). In these cases the single objects are too small to be reconstructed from the degraded image.

3.3. Forest case study

In a third case study the use of AIF was tested for a forest application. The objective was the derivation of a forest mask from Landsat TM imagery in combination with a panchromatic SPOT image in an alpine region. The two images were acquired on August 18, 1992 and August 17, 1992 respectively. The area is located in the center of Austria, in the Dachstein region, Styria (centered on 13°40'E / 47°20'N). Both images were

(a)

(b)

(c)

Fig. 4. Fusion of ATM image data. (a) original image (6m), © ÖBIG 1991. (b) degraded image (18m). (c) AIF image (6m).

geocoded with respect to a digital terrain model in the Austrian reference system, thus no geometric distortions appear between the images.

The derivation of the forest mask is based on thresholding of the single Landsat TM image bands. Applying this technique on the original image bands leads to a reliable forest mask, however the geometric resolution of this mask is limited by the pixel size of 30m. On the other hand, the panchromatic image that would provide the better spatial resolution does not offer the spectral information needed to separate the forest areas from other land cover objects. The fusion of both data sets was expected to result in an improved forest mask.

The AIF was applied to the two data sets using a window size of 15 x 15, 7 iterations and a variance decreasing iteratively from 0.025 to 0.01. Next the thresholding technique was applied to the resulting multispectral fusion product using the same thresholds as for the original Landsat TM bands. As expected, the resulting forest mask delineates the forest areas significantly better.

Fig. 5 shows the two vectorised forest masks superimposed to an aerial colour infrared photograph of the area. Visual evaluation of the results shows the improvement gained from the fusion approach. The borderlines of the forest mask are smoother and follow the actual border of the forest areas. Due to the pre-segmentation effect of the AIF, only areas of a certain minimum crown coverage are recognized as forest.

4. SUMMARY AND CONCLUSIONS

The case studies demonstrated the benefits and limitations of the AIF algorithm. The AIF was designed as a pre-processing tool for subsequent numerical classification. Its advantage lies in the pre-segmentation of the fused image, resulting in a low variance within the objects and sharp borders between the objects. The inclusion of highly textured areas from the panchromatic image is not supported by the technique, but the spectral characteristics of the multispectral image are preserved to a high extent.

The first case study demonstrated the use of AIF for agricultural applications. Objects of interest are the single fields that represent the different agricultural crops of the area. These objects are expected to be of such a size that their spectral characteristics are represented even by the lower resolution of the multispectral image. Application of AIF improves a subsequent classification by sharpening the borders of the fields, thus reducing the number of mixed pixels and allowing for a more precise estimation of the actual areas covered by the single crop types.

The urban case study proved the applicability of AIF to very high spatial resolution multispectral data. By degrading the multispectral image to a lower spatial resolution and fusing the result with an artificial panchromatic image, a comparison

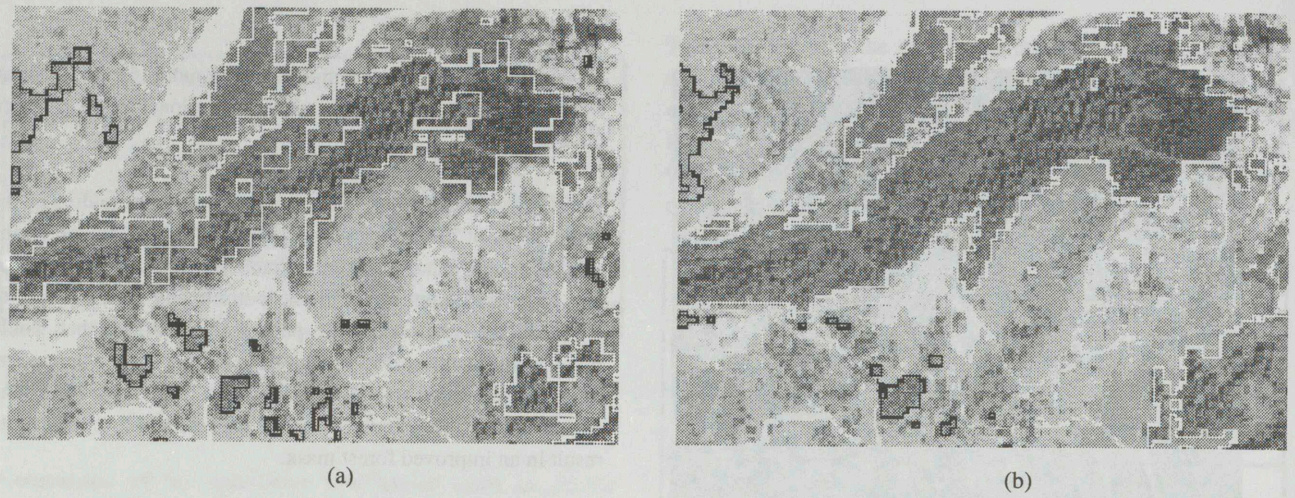

(a) (b)

Fig. 5. Overlay of vectorised forest masks to aerial reference image, © BEV 1992. (a) Forest mask derived from Landsat TM image. (b) Forest mask derived from AIF image, © Joanneum Research 1999.

between the fusion results and the "true" image could be performed. The evaluation proved the spectral stability of the algorithm and the higher correlation between the "true" and the fused image compared to the degraded image.

The third case study showed the application of AIF to multisensor image data acquired by Landsat TM and SPOT PAN. The objective was the derivation of a forest mask using a threshold technique. While the thresholding of the Landsat TM bands provided a reliable mask, the shape of this mask could be significantly improved by first applying the AIF to the multispectral bands and the panchromatic image.

The conclusions drawn from the application in the test sites are manifold. The AIF is considered useful for areas that are dominated by objects larger than the low resolution pixel size. Taking the average pixel size of current multispectral sensors this prerequisite is only true for certain types of image objects, such as agricultural fields. However, with the increasing spatial resolution of the new sensor generation, this limitation will become less and less important. On the contrary, the application of AIF might help to reduce the enormous complexity of very high resolution images. In cases of small objects that do not benefit from the AIF, we suggest to use the fusion result for first level classification, i.e. classification of meta-classes that provide image masks for subsequent detailed classification. The advantage of this approach lies in the sharper delineation of the meta-objects, thus leading to less misclassifications caused by mixed pixels.

A final suggestion refers to the combination of AIF and substitution techniques for visualisation. AIF would first sharpen object edges and thus eliminate the blocky pixel structure of the low resolution image. Then the local texture could be added by applying a substitution technique onto the AIF processed image, thus leading to a sharpened high resolution multispectral image product. However, this product is not considered an appropriate input for numerical classification but offers an improved basis for visual interpretation of the image.

ACKNOWLEDGEMENTS

Part of this work has been supported by the European Commission, Contract No. ENV4-CT96-0359. The author thanks W. Pillmann (ÖBIG) for providing the ATM data of Vienna. The contribution of Ursula Schmitt (Joanneum Research) to the forest case study is greatfully acknowledged.

REFERENCES

Benediktsson J.A. and Swain P.H. 1992. Consensus theoretic classification methods. IEEE Trans. Syst., Man, Cybern., 22(4), pp. 688-704.

Carlson G.R. and Patel B. (1997): A new area dawns for geo-spatial imagery. GIS World, 10(3), pp. 36-40.

Carper W.J., Lillesand T.M. and Kiefer R.W., 1990. The use of intensity-hue-saturation transformation for merging SPOT panchromatic and multispectral image data. Photogrammetric Eng. Remote Sensing, 56(4), pp. 459-467.

Chavez P.S., Sides S.C. and Anderson J.A., 1991. Comparison of three different methods to merge multiresolution and multispectral data: Landsat TM and SPOT panchromatic. Photogrammetric Eng. Remote Sensing, 57(3), pp. 295-303.

Janssen L.L., Jaarsma M.N. and van der Linden E.T., 1990. Integrating topographic data with remote sensing for land-cover classification. Photogrammetric Eng. Remote Sensing, 56(11), pp. 1503-1506.

Garguet-Duport B., Girel J., Chassery J.-M., Pautou G., 1996. The use of multiresolution analysis and wavelet transform for merging SPOT panchromatic and multispectral image data. Photogrammetric Eng. Remote Sensing, 62(9), pp. 1057-1066.

Harris J.R., Murray R. and Hirose T., 1990. IHS Transform for the integration of radar imagery with other remotely sensed data. Photogrammetric Eng. Remote Sensing, 56(12), pp. 1631-1641.

Kressler F. and Steinnocher K., 1996. Change detection in urban areas using satellite data and spectral mixture analysis. In: International Archives of Photogrammetry and Remote Sensing, Vol. 31, Part B7, pp. 379-383.

Lee J. S., 1983. A simple speckle smoothing algorithm for synthetic aperture radar images. IEEE Trans. Syst. Man, Cybern., 13, pp. 85-89.

Lillesand T.M. and Kiefer R.W., 1994. Remote sensing and image interpretation. New York: John Wiley and Sons.

Pellemans A.H.J.M., Jordans R.W.L. and Allewijn R., 1993. Merging multispectral and panchromatic SPOT images with respect to the radiometric properties of the sensor. Photogrammetric Eng. Remote Sensing, 59(1), pp. 81-87.

Pohl C. and Van Genderen J.L., 1998. Multisensor image fusion in remote sensing: concepts, methods and applications. Int. J. Remote Sensing, 19(5), pp. 823-854.

Rachin T. and Wald L., 1993. The wavelet transform for the analysis of remotely sensed images. Int. J. Remote Sensing, 14(3), pp. 615-619.

Schistad Solberg A.H., Jain A.K. and Taxt T., 1994. Multisource classification of remotely sensed data: fusion of Landsat TM and SAR images. IEEE Trans. Geosci. Remote Sensing, 32(4), pp. 768-778.

Shettigara V.K., 1992. A generalized component substitution technique for spatial enhancement of multispectral images using a higher resolution data set. Photogrammetric Eng. Remote Sensing, 58(5), pp. 561-567.

Singh A., 1989. Digital change detection techniques using remotely-sensed data. Int. J. Remote Sensing, 10(6), pp. 989-1003.

Smith D.M., 1996. Speckle reduction and segmentation of synthetic aperture radar images. Int. J. Remote Sensing, 17(11), pp. 2043-2057.

Van Genderen J.L. and Pohl C., 1994. Image fusion: issues, techniques and applications. Proc. EARSeL Workshop Intelligent Image Fusion, J. L. Van Genderen and V. Cappellini (Eds.), Strasbourg, France, September.

Vrabel J., 1996. Multispectral imagery band sharpening study. Photogrammetric Eng. Remote Sensing, 62(9), pp. 1075-1083.

Wald L., Ranchin T. and Mangolini M., 1997. Fusion of satellite images of different spatial resolutions: assessing the quality of resulting images. Photogrammetric Eng. Remote Sensing, 63(6), pp. 691-699.

Weydal D.J., 1993. Multitemporal analysis of ERS-1 SAR images over land areas. Proc. IEEE Symp. Geosci. Remote Sensing (IGARSS'93), Tokyo, Japan, pp. 1459-1461.

Yocky D.A., 1996. Multiresolution wavelet decomposition image merger of Landsat Thematic Mapper and SPOT panchromatic data. Photogrammetric Eng. Remote Sensing, 62(9), pp. 1067-1074.

Zhukov B., Berger M., Lanzl F. and Kaufmann H., 1995. A new technique for merging multispectral and panchromatic images revealing sub-pixel spectral variation. Proc. IEEE Symp. Geosci. Remote Sensing (IGARSS'95), Florence, Italy, pp. 2154-2156.